

**Molecular oxygen tetramer (O<sub>2</sub>)<sub>4</sub>: Intermolecular interactions and implications for the  $\epsilon$  solid phase**

Massimiliano Bartolomei,\* Estela Carmona-Novillo, Marta I. Hernández, Jesús Pérez-Ríos, and José Campos-Martínez  
*Instituto de Física Fundamental, Consejo Superior de Investigaciones Científicas (IFF-CSIC), Serrano 123, ES-28006 Madrid, Spain*

Ramón Hernández-Lamonedá

*Centro de Investigaciones Químicas, Universidad Autónoma del Estado de Morelos, 62210 Cuernavaca, Mor. México*

(Received 13 July 2011; published 22 September 2011)

Recent data have determined that the structure of the high-pressure  $\epsilon$  phase of solid oxygen consists of clusters composed of four O<sub>2</sub> molecules. This finding has opened the question about the nature of the intermolecular interactions within the molecular oxygen tetramer. We use multiconfigurational *ab initio* calculations to obtain an adequate characterization of the ground singlet state of (O<sub>2</sub>)<sub>4</sub>, which is compatible with the nonmagnetic character of the  $\epsilon$  phase. In contrast to previous suggestions implying covalent bonding, we show that (O<sub>2</sub>)<sub>4</sub> is a van der Waals-like cluster where exchange interactions preferentially stabilize the singlet state. Nevertheless, as the cluster shrinks, there is an extra stabilization due to many-body interactions, i.e., an incipient chemical bonding that just yields a softening of the repulsive wall. We show that these findings can be used to model the intra- and intercluster distances of  $\epsilon$ -O<sub>2</sub> observed in the lower-pressure range and are consistent with inelastic x-ray measurements of O<sub>2</sub> K-edge excitations.

DOI: 10.1103/PhysRevB.84.092105

PACS number(s): 36.40.-c, 31.15.aa, 34.20.Gj, 62.50.-p

Recently, the determination of the structure of the high pressure  $\epsilon$  phase of oxygen<sup>1,2</sup> has raised interest in the study of molecular oxygen oligomers. In contrast to previously proposed structures based on the dimer<sup>3</sup> and herringbone chains,<sup>4</sup> two independent x-ray diffraction experiments<sup>1,2</sup> definitively concluded that  $\epsilon$ -O<sub>2</sub> consists of layers of well defined (O<sub>2</sub>)<sub>4</sub> aggregates. They were found to form prisms with the O<sub>2</sub> axes perpendicular<sup>1</sup> or nearly perpendicular<sup>2</sup> to a rhombic, nearly squared, base. There is a hierarchy of distances in this phase, the O<sub>2</sub> bond length, which nearly keeps the gas phase value ( $\approx 1.21$  Å) at all pressures, and the intra- and intercluster distances (2.34 and 2.66 Å at 11.4 GPa), which decrease monotonically with pressure up to the boundary with the metallic  $\zeta$  phase.<sup>2</sup> Other key properties of this phase, suggesting increasing intermolecular interactions, are a dark-red color, a strong infrared absorption, and a magnetic collapse.<sup>3,5-7</sup> Further evidence for a different intermolecular bonding has come from inelastic x-ray scattering<sup>8</sup> where, at the lower pressure boundary of this phase (10 GPa), a discontinuous shift of about 1.1 eV in the electronic transitions from  $1s$  to  $1\pi_g^*$  orbitals was found.

A few works<sup>1,9-11</sup> have attempted to rationalize the stability and the bonding of the (O<sub>2</sub>)<sub>4</sub> species in the framework of the density functional theory (DFT), but with unclear results. Thus, authors of Ref. 9 found that the  $D_{4h}$  cuboid structure corresponds to a local energy minimum that they recognized as unstable when higher levels of theory were applied. Furthermore, DFT calculations in Ref. 10 failed to show that the experimental (O<sub>2</sub>)<sub>4</sub> geometry is the most stable one compared with other chain structures,<sup>4</sup> showing the need for additional studies. Then, it is apparent that despite recent progress<sup>12-14</sup> made in DFT methodologies for treating dispersion forces, the multiconfigurational character of molecular oxygen clusters in low-spin multiplicity states still remains a serious problem for such techniques.

As a matter of fact the nature of the bonding in such molecular clusters has been a subject of debate for several decades. A chemically bound dimer was expected considering

the open shell  $^3\Sigma_g^-$  character of O<sub>2</sub> where two unpaired electrons occupy degenerate  $\pi_g^*$  orbitals. However, a number of experimental<sup>15-17</sup> and theoretical<sup>18-20</sup> works clarified that in the gas phase, (O<sub>2</sub>)<sub>2</sub> has the typical features of a van der Waals complex: a well depth of tens of meV and retention of the molecular properties within the complex. In fact, it has been shown<sup>18,19</sup> that a singlet species of  $D_{2h}$  symmetry is stabilized due to exchange interactions but not in a sufficient extent to lead to chemical bonding.

We report here high level supermolecular *ab initio* calculations of the (O<sub>2</sub>)<sub>4</sub> cluster. Our goal is a reliable characterization of the singlet ground state, which is consistent with the magnetic collapse<sup>7</sup> and spectroscopy<sup>3,5,6</sup> of the  $\epsilon$  phase. To this end, we use a multiconfigurational ansatz, which is unavoidable for spin multiplicities of (O<sub>2</sub>)<sub>4</sub> lower than the maximum one (nonet). We proceed in analogy to our previous work on the dimer<sup>19,20</sup> and treat the highest spin complex by means of a restricted coupled cluster theory with singles, doubles, and perturbative triple excitations [RCCSD(T)]. In addition, the singlet-nonnet splitting can be well described at the multiconfigurational complete active space second-order perturbation (CASPT2) theory. Finally, the (O<sub>2</sub>)<sub>4</sub> singlet energy is obtained by adding to the RCCSD(T) nonet potential the singlet-nonnet CASPT2 splitting. The aug-cc-pVQZ<sup>21</sup> basis set has been used at all levels of theory. For the CASPT2 calculations, the active space is defined by distributing eight electrons in eight molecular orbitals correlating asymptotically with the O<sub>2</sub>  $\pi_g^*$  shell. As customary, these orbitals have been previously optimized with the complete active space self-consistent field (CASSCF) method. The counterpoise method<sup>22</sup> was applied to correct interaction energies for the basis set superposition error. As for the (O<sub>2</sub>)<sub>4</sub> geometry, we use a cuboid structure with  $D_{4h}$  symmetry. The centers of mass of O<sub>2</sub> form a square whose side is changed in the range 1.5–25 Å, while the intramolecular distance is kept fixed to 1.2065 Å. Calculations have been performed with the MOLPRO2006.1 package.<sup>23</sup> To study the role of many-body interactions, we compare the supermolecular calculations with

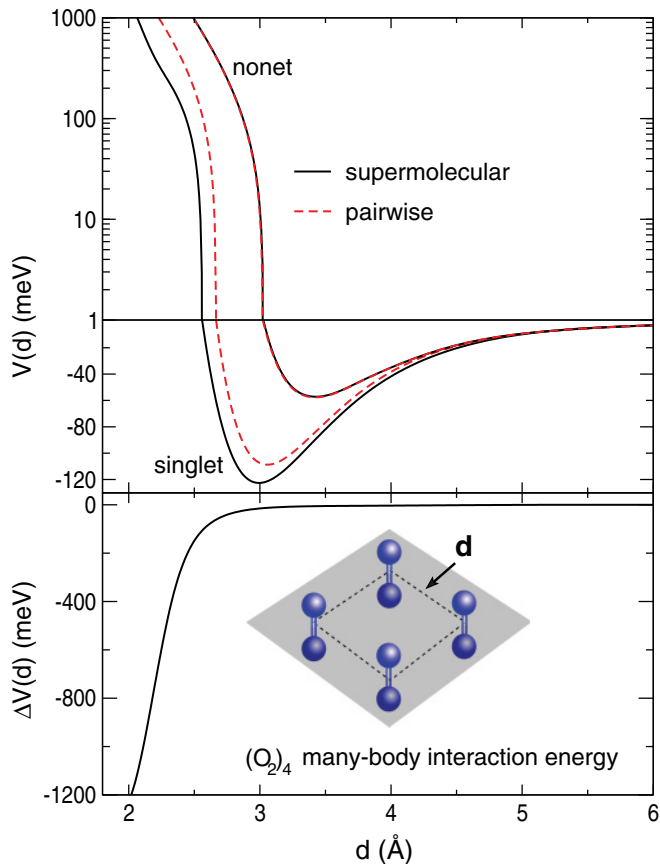


FIG. 1. (Color online) Upper panel: interaction energies (in meV) for the nonet and ground singlet states of  $(\text{O}_2)_4$  as functions of the square side  $d$  (in Å). Supermolecular approach is represented in solid lines while the pairwise approach in dashed lines. Lower panel: many-body interaction energy for the singlet state  $\Delta V(d)$  obtained as the difference between supermolecular and pairwise energies. The large values of  $\Delta V$  at small  $d$ 's might be a key feature to explain the clustering of  $\text{O}_2$  molecules in the  $\epsilon$  phase.

estimations based on the summation of pure pair interactions obtained at the same level of theory as those of  $(\text{O}_2)_4$ . In the pairwise approach, we have obtained expressions for the  $(\text{O}_2)_4$  energy that are compatible with a well-defined total spin of the complex. It must be noted that there are three singlet states<sup>24</sup> asymptotically correlating with four  $\text{O}_2(^3\Sigma_g^-)$ , and that here, we are reporting the calculations of the ground singlet state.

The interaction energies of  $(\text{O}_2)_4$  in the singlet and nonet states as functions of the square side  $d$  are reported in the upper panel of Fig. 1 together with the pairwise estimations of the corresponding interactions. Equilibrium parameters of these potentials are given in Table I. As can be seen from the parameters of the singlet and nonet potential wells,  $(\text{O}_2)_4$  is a van der Waals-like complex in the gas phase, mainly stabilized by dispersion interactions. The exchange interaction, however, plays a role making the potential well of the singlet state deeper and shifted at shorter intermolecular distances than that of the nonet state. As in the dimer,<sup>19,20</sup> the exchange interaction favors the states of lowest spin multiplicity.

More insight is gained when comparing the supermolecular calculations with the pairwise estimations. For the nonet state, the pairwise approximation reproduces very well the

TABLE I. Binding energy  $D_e$  (in meV) and equilibrium distance  $R_e$  (in Å) of the  $(\text{O}_2)_4$  potentials reported in Fig. 1.

	nonet		singlet	
	$D_e$	$R_e$	$D_e$	$R_e$
supermolecular	56.6	3.37	122.6	2.99
pairwise	57.1	3.37	108.4	3.08

supermolecular energies indicating that many-body effects are not particularly relevant. However, for the singlet state, an analogous agreement is only achieved for the largest  $d$  sizes of the cluster. Around the minimum of the singlet well, the supermolecular energies are already lower than the pairwise ones (see Table I), but it is for shorter distances where a remarkable softening of the repulsive wall is found. This is due to a many-body effect, as shown in the lower panel of Fig. 1 where it can be noticed that the many-body interaction energy for the singlet state increases dramatically as  $d$  decreases, being about 1.2 eV at  $d = 2$  Å. The origin of this effect must be in the exchange interactions,<sup>25</sup> since polarization contributions to many-body interaction energies, if important, should be shown also for the nonet state, which is not the case.

In a molecular crystal, the first response to pressure is a “squeezing out of van der Waals space,” in other words, the penetration to the repulsive region of the intermolecular potentials.<sup>26</sup> Therefore the peculiar behavior at short cluster sizes is relevant indeed for understanding the structure of the high-pressure  $\epsilon$  phase,<sup>1,2</sup> as is discussed in the following.

Some clues for the softening of the repulsive wall of the ground singlet state are given in Fig. 2, where we show CASSCF molecular orbitals arising from the interaction of the eight half-occupied  $\pi_g^*$  orbitals of  $\text{O}_2$ . An analogous calculation for singlet  $(\text{O}_2)_2$  is shown for the sake of comparison. The properties of these optimized orbitals barely change from the asymptote up to the equilibrium distance ( $d \approx 3$  Å), but for shorter  $d$ 's the interaction does give rise to bonding and antibonding orbitals. Interestingly, the four bonding orbitals in  $(\text{O}_2)_4$  are more stable than the bonding orbitals of  $(\text{O}_2)_2$  and the associated occupation numbers increase faster as  $d$  decreases, as a result of many-body exchange effects. However, a double occupancy only occurs for very short distances ( $d < 1.8$  Å). Moreover, the  $(\text{O}_2)_4$  orbital stabilization is much smaller than the electron-electron Coulomb repulsion contribution to the total interaction. Thus the result is an incipient chemical bonding leading not to a minimum but just to a softening of the repulsive region of the potential, as shown in Fig. 1. This multiconfigurational analysis differs from those of Refs. 9 and 8 where, based on a simpler monoconfigurational picture, it was suggested that all the bonding orbitals were doubly occupied leading to large binding energies with respect to the isolated  $\text{O}_2$  molecules. The present analysis also gives a qualitative insight into the observation of a  $\approx 1$ -eV shift in the  $\pi_g^* \leftarrow 1s$  transitions at the boundary of the  $\epsilon$  phase,<sup>8</sup> since the splitting between the  $(\text{O}_2)_4$  antibonding energies and the isolated  $\pi_g^*$  orbitals is of the same order of magnitude ( $\approx 1.5$  eV) in the relevant range ( $d \approx 2.4$  Å).

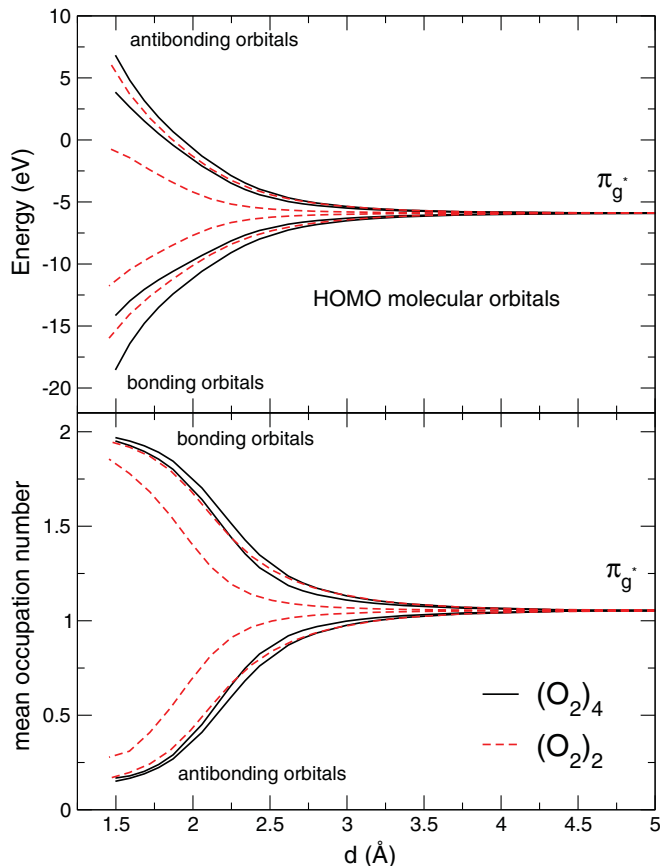


FIG. 2. (Color online) Upper panel: energies of the HOMOs originated from the  $O_2 \pi_g^*$  orbitals vs intermolecular distance  $d$ , for the ground singlet states of  $(O_2)_4$  and  $(O_2)_2$ . Note that for the tetramer, each line corresponds to a couple of almost degenerate HOMOs. Lower panel: as in the upper panel but for the occupation numbers.

In order to study whether the present results are adequate for a description of the  $\epsilon$  phase, we consider a very simple model for the energy of a layer of  $(O_2)_4$  clusters, with the  $O_2$  interatomic distance kept fixed.<sup>27</sup> A basic unit cell is shown in Fig. 3 where the tetramers form rhombuses of length  $d$  and angle  $\alpha$ . It is assumed that, at a given pressure, the centers of mass of the clusters are fixed and determined by the lattice parameters  $a$  and  $b$ . Values of these parameters as functions of pressure were taken from Ref. 2. In addition, the angle  $\alpha$  is fixed to  $81.4^\circ$  as derived from data reported at 11.4 GPa.<sup>2</sup> We assume that all clusters increase/decrease their size  $d$  at a time and study the subsequent modification of the cell energy. This energy is given as a sum of intra and intercluster contributions

$$E(d) = V^{\text{intra}}(d) + \frac{1}{2} \sum_{i,j} V_{ij}^{\text{inter}}(r_{ij}), \quad (1)$$

where  $V^{\text{intra}}$  is the supermolecular  $(O_2)_4$  singlet potential and  $V_{ij}^{\text{inter}}$  is a pair potential between molecules  $i$  and  $j$  belonging to different clusters. The corresponding intermolecular distance  $r_{ij}$  is determined by  $d$ ,  $a$ ,  $b$ , and  $\alpha$ . A spin-averaged  $(O_2)_2$  potential was used for  $V_{ij}^{\text{inter}}$  because the nonmagnetic character<sup>7</sup> of the  $\epsilon$  phase suggests that the dependence on spin must be washed out. In Fig. 3 (upper panel), it is shown that,

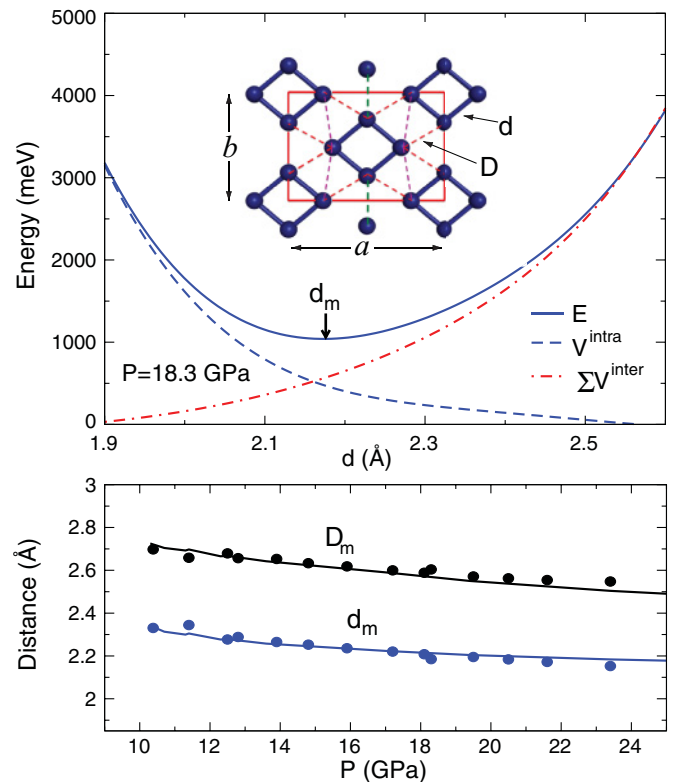


FIG. 3. (Color online) Upper panel: energy of a layer of  $\epsilon$ - $O_2$  [Eq. (1)] as a function of the cluster size,  $d$ , for a pressure of 18.3 GPa (solid line). In the inset, the model unit cell is shown where the  $O_2$  axes are perpendicular to the  $a$ - $b$  plane and the intercluster distances,  $r_{ij}$ , are displayed by dashed lines,  $D$  being the shortest one among them. A minimum of the energy is obtained for the intracuster distance  $d_m$ . Lower panel: Pressure dependence of  $d_m$  and  $D_m$  (lines) compared with data of Ref. 2 (circles). See text for details.

within the cell, the optimum size of the cluster is considerably reduced with respect to the gas phase equilibrium distance. For 18.3 GPa, a minimum in the total energy is obtained at about  $d_m = 2.17 \text{ \AA}$ , in agreement with the observed intracuster distance of  $2.185 \text{ \AA}$ <sup>2</sup> and with the value obtained at 17.6 GPa in another independent experiment.<sup>1</sup> In the lower panel of Fig. 3, we show that the pressure dependence of the optimized intra and intercluster distances  $d_m$  and  $D_m$  agrees fairly well with the observations<sup>2</sup> ( $D_m$  is the shortest intercluster distance, obtained as a function of  $d_m$ ,  $a$ ,  $b$ , and  $\alpha$ ) for pressures lower than 20–25 GPa.

We would like to stress that, despite the simplicity of the model, the key element is the behavior of the repulsive wall of the ground singlet state, adequately calculated at a multiconfigurational level of theory. Indeed, substitution of the ground singlet energy  $V^{\text{intra}}(d)$  with that obtained at a lower level of theory<sup>28</sup> would lead to an optimum intracuster size far less compatible with the measurements. As discussed in Ref. 1, the fact that both intra and intercluster distances compress at nearly the same rate is a clear indication of a rather weak interaction between the  $O_2$  molecules. We believe that the present findings of a van der Waals cluster with an incipient chemical bond for short sizes will be a key ingredient in future rationalization and modeling of the structure of  $\epsilon$ -oxygen as

well as the pressure dependence of its vibrational modes. As an example, the pressure dependence<sup>3</sup> of the IR vibron frequency displays a minimum at about 20 GPa suggesting a change in the O<sub>2</sub> interatomic distance. This behavior, already observed in other molecular crystals,<sup>29</sup> should be interpreted and taken into account in more detailed analyses.

We thank Yuichi Akahama for sending us structural data of Ref. 2 and funding by MICINN (Spain, FIS2010-22064-C02-02). R.H.L. was supported by a sabbatical grant by MEC (Spain, SAB2009-0010) and Conacyt (Mexico, Ref. 126608). J.P.-R. is a pre-JAE CSIC fellow. We thank Nestor A. Aguirre for assistance in the preparation of the figures.

\*maxbart@iff.csic.es

<sup>1</sup>L. F. Lundegaard, G. Weck, M. I. McMahon, S. Desgreniers, and P. Loubeyre, *Nature (London)* **443**, 201 (2006).

<sup>2</sup>H. Fujihisa, Y. Akahama, H. Kawamura, Y. Ohishi, O. Shimomura, H. Yamawaki, M. Sakashita, Y. Gotoh, S. Takeya, and K. Honda, *Phys. Rev. Lett.* **97**, 085503 (2006).

<sup>3</sup>F. A. Gorelli, L. Ulivi, M. Santoro, and R. Bini, *Phys. Rev. B* **63**, 104110 (2001).

<sup>4</sup>J. B. Neaton and N. W. Ashcroft, *Phys. Rev. Lett.* **88**, 205503 (2002).

<sup>5</sup>Y. A. Freiman and H. J. Jodl, *Phys. Rep.* **401**, 1 (2004).

<sup>6</sup>Y. Akahama and H. Kawamura, *Phys. Rev. B* **61**, 8801 (2000).

<sup>7</sup>I. N. Goncharenko, *Phys. Rev. Lett.* **94**, 205701 (2005).

<sup>8</sup>Y. Meng, P. J. Eng, J. S. Tse, D. M. Shaw, M. Y. Hu, J. Shu, S. A. Gramsch, C. Kao, R. J. Hemley, and H. K. Mao, *Proc. Natl. Acad. Sci. USA* **105**, 11640 (2008).

<sup>9</sup>R. Steudel and M. W. Wong, *Angew. Chem. Int. Ed.* **46**, 1768 (2007).

<sup>10</sup>B. Militzer and R. J. Hemley, *Nature (London)* **443**, 150 (2006).

<sup>11</sup>Y. Ma, A. R. Oganov, and C. W. Glass, *Phys. Rev. B* **76**, 064101 (2007).

<sup>12</sup>A. Becke and E. Johnson, *J. Chem. Phys.* **127**, 124108 (2007).

<sup>13</sup>E. Johnson, S. Keinan, P. Mori-Sánchez, J. Contreras-García, A. Cohen, and W. Yang, *J. Am. Chem. Soc.* **132**, 6498 (2010).

<sup>14</sup>J. Toulouse, I. C. Gerber, G. Jansen, A. Savin, and J. G. Angyan, *Phys. Rev. Lett.* **102**, 096404 (2009).

<sup>15</sup>C. Long and G. Ewing, *J. Chem. Phys.* **58**, 4824 (1973).

<sup>16</sup>L. Biennier, D. Romanini, A. Kachanov, A. Campargue, B. Bussery-Honvault, and R. Bacis, *J. Chem. Phys.* **112**, 6309 (2000).

<sup>17</sup>V. Aquilanti, D. Ascenzi, M. Bartolomei, D. Cappelletti, S. Cavalli, M. de Castro Vitores, and F. Pirani, *Phys. Rev. Lett.* **82**, 69 (1999).

<sup>18</sup>P. Wormer and A. van der Avoird, *J. Chem. Phys.* **81**, 1929 (1984).

<sup>19</sup>M. Bartolomei, M. I. Hernández, J. Campos-Martínez, E. Carmona-Novillo, and R. Hernández-Lamonedá, *Phys. Chem. Chem. Phys.* **10**, 5374 (2008).

<sup>20</sup>M. Bartolomei, E. Carmona-Novillo, J. Campos-Martínez, M. I. Hernández, and R. Hernández-Lamonedá, *J. Chem. Phys.* **133**, 12431 (2010).

<sup>21</sup>R. Kendall, J. T. H. Dunning, and R. Harrison, *J. Chem. Phys.* **96**, 6796 (1992).

<sup>22</sup>J. van Lenthe, J. van Duijneveldt-van de Rijdt, and F. van Duijneveldt, *Adv. Chem. Phys.* **69**, 521 (1987).

<sup>23</sup>H.-J. Werner *et al.*, MOLPRO, version 2006.1, a package of *ab initio* programs (2006) [<http://www.molpro.net>].

<sup>24</sup>H. V. Gomonay and V. M. Loktev, *Phys. Rev. B* **76**, 094423 (2007).

<sup>25</sup>C. C. Díaz-Torrejón and I. G. Kaplan, *Chem. Phys.* **381**, 67 (2011).

<sup>26</sup>W. Grochala, R. Hoffmann, J. Feng, and N. W. Ashcroft, *Angew. Chem. Int. Ed.* **46**, 3620 (2007).

<sup>27</sup>The determination of the O<sub>2</sub> interatomic distance at 17.6 GPa<sup>1</sup> together with the IR and Raman profiles of Refs. 3 and 6 suggest just small changes (few percent) of the O<sub>2</sub> interatomic distance in the 10–25 GPa pressure range.

<sup>28</sup>Hartree-Fock, CASSCF, and DFT (with the B3LYP and PW91 functionals) calculations have been performed to obtain the corresponding  $V^{\text{intra}}$  and  $V^{\text{inter}}$  potentials.

<sup>29</sup>A. San-Miguel, H. Libotte, M. Gauthier, G. Aquilanti, S. Pascarelli, and J. P. Gaspard, *Phys. Rev. Lett.* **99**, 015501 (2007).